ELSEVIER

Catalysis Today 59 (2000) 395–402

CATALYSIS TODAY

www.elsevier.com/locate/cattod

Thermal aging of Pd/Pt/Rh automotive catalysts under a cycled oxidizing–reducing environment

Juan R. González-Velasco*, Juan A. Botas, Raquel Ferret, M. Pilar González-Marcos, Jean-Louis Marc, Miguel A. Gutiérrez-Ortiz

Department of Chemical Engineering, Faculty of Sciences, Universidad del País Vasco/EHU, PO Box 644, E-48080 Bilbao, Spain

Abstract

Mono- and multi-metallic (bi- and tri-) Pt, Pd and Rh supported on cerium-promoted alumina (La Roche, SAS-1/16) catalysts were tested for activity as TWC, both fresh [G.C. Koltsakis, and A.M. Stamatelos, Progr. Energy Combust. Sci. 23 (1997) 1] and after accelerated aging. Aging consisted of a treatment at 900°C for 5 h during which an oxidizing (2.5% O_2, 10% H_2O, in N_2) and a reducing (5.0% CO, 10% H_2O, in N_2) feedstream were cycled at 0.017 Hz through the catalyst. Activity tests were carried out by increasing temperature from 100 to 600°C at 3°C min^{-1}, while two oxidizing and reducing ($\pm$0.5 *A*/*F*) feedstreams were alternately (1 Hz) fed through the reactor at 125 000 h^{-1} (STP). Conversion was continuously analyzed. Light-off temperature, T_{50}, conversion at 500°C (normal running temperature), X_{500}, and the stoichiometric window (*A*/*F* from 14.13 to 15.13) for stationary feedstreams, were determined. © 2000 Elsevier Science B.V. All rights reserved.

Keywords: Automotive exhaust control; TWC; Aging; Platinum; Palladium; Rhodium

1. Introduction

Regulations concerning automotive emissions are becoming more and more stringent every day (Directive 98/69/EC of the European Parliament and of the Council of October 13, 1998). This makes it necessary to develop more efficient and resistant catalytic systems, which can endure the severe conditions in the catalytic converter during normal operation.

Three-way catalysts (TWC), performing simultaneous oxidation of carbon monoxide (CO) and hydrocarbons (HC) and reduction of nitrogen oxides (NO_x), seem to be, up to now, a satisfactory and efficient solution. An overview of the advanced technologies currently used for abating emissions from internal combustion engines can be found in the literature [1,2].

Optimal operation of these catalysts requires a composition of the exhaust gaseous stream around the stoichiometric air-to-fuel ratio, *A*/*F*=14.63, which should be precisely controlled. Resistance to thermal aging is one of the main concerns when studying catalyst life, as the catalyst may be subjected to high temperatures (up to 1000°C) in an environment with a high steam content (up to 10%) and variable redox character during normal operation in the catalytic converter. Thus, resistance to thermal aging must be maximized in order to increase the durability of the catalyst.

Deactivation can be due to sintering of the metal particles and change in the interactions between the different components or metal encapsulation. Also, the loss of ceria surface area due to particle growing can directly influence its oxygen storage capacity, which

* Corresponding author.
E-mail address: iqpgovej@lg.ehu.es (J.R. González-Velasco)

0920-5861/00/$ – see front matter © 2000 Elsevier Science B.V. All rights reserved.
PII: S0920-5861(00)00304-7

is a fundamental parameter to increase the catalyst efficiency.

Previously, we had studied the performance of fresh Pd, Pt, Rh, Pd–Pt, Pd–Rh, Pt–Rh and Pd–Pt–Rh catalysts as TWC in a simulated stationary and/or cycled environment similar to that existing in automobile catalytic converters [3]. Comparison of the activity obtained with multi-metallic catalysts prepared by co-adsorption and those obtained with physical mixtures of mono-metallic catalysts has allowed the study of the interactions between noble metals in multi-metallic catalysts prepared by co-adsorption.

In this work, we have subjected the previous mono- and multi-metallic catalysts to accelerated thermal aging in cycled (oxidizing–reducing) feedstream. Then, the performances of fresh and aged samples have been compared and analyzed.

2. Experimental

2.1. Materials

The starting alumina was SAS-1/16 supplied by La Roche. After grinding to adequate particle size and calcination in air at 700°C for 4 h, its properties resulted as shown in Table 1.

Ceria was incorporated by the conventional incipient wetness method from an $Ce(NO_3)_3{\cdot}nH_2O$ aqueous solution, at 40°C and 30 mm Hg. Promoter-modified alumina samples were dried at 120°C for 2 h and calcined in air at 700°C for 4 h in order to decompose the nitrate to oxide.

The active phases, Pd, Pt, and Rh, were incorporated by adsorption from aqueous solution of their corresponding salts, $PdCl_2$, $H_2PtCl_6{\cdot}nH_2O$, and $RhCl_3{\cdot}nH_2O$, using 40 cm^3 of solution per gram of ceria-modified alumina. The multi-metallic catalysts were prepared by joint adsorption of the corresponding metallic salts — Pd–Pt, Pd–Rh, Pt–Rh, and Pd–Pt–Rh. The nominal composition of the prepared catalysts was 0.5 wt.% Pd, 0.1 wt.% Pt, and 0.02 wt.% Rh. After drying in nitrogen for 1 h at 120°C, final activation of the precursors was made by calcination at 550°C in nitrogen for 4 h and subsequent treatment in 10% H_2/N_2 for additional 2 h. The final catalysts resulted in the compositions shown in Table 2, determined by atomic absorption spectroscopy (AAS).

Table 1
Properties of the alumina after calcination in air at 700°C for 4 h

Catalyst size (mm)	0.5–1.0
Surface area BET ($m^2\,g^{-1}$)	200
Pore volume ($cm^3\,g^{-1}$)	1.0
Average pore radius (nm)	5.3
Mode pore radius (nm)	6.1
Isoelectric point	7.6

Table 2
Composition of the prepared catalysts (wt.%)

Component	CeO_2	Pd	Pt	Rh
Mono-metallic catalysts				
Pd	7.29	0.47	–	–
Pt	8.83	–	0.079	–
Rh	8.84	–	–	0.021
Multi-metallic catalysts				
Pd–Pt	8.43	0.45	0.088	–
Pd–Rh	8.81	0.47	–	0.017
Pt–Rh	9.16	–	0.081	0.021
Pd–Pt–Rh	8.87	0.50	0.087	0.017

2.2. Aging procedure

The fresh catalysts were severely aged at 900°C for 5 h in an environment obtained by cycling, with a frequency of 0.017 Hz, the following feedstreams:

- oxidizing feedstream — 2.5% O_2, 10% H_2O, balance of N_2;
- reducing feedstream — 5% CO, 10% H_2O, balance of N_2.

After the treatment, the catalysts were cooled down to room temperature under the same environment and finally the stream was shifted to nitrogen.

2.3. Activity tests

Catalytic activity data of fresh and aged catalysts were obtained in a stainless steel, 12 mm internal diameter tubular reactor with a fixed-bed of catalyst (3.5 cm^3, ca. 1.8 g) at atmospheric pressure [4]. The catalytic bed was placed on ceramic wall at the lower part of the reactor. Above the catalyst, a bed of 10 cm^3 of inactive ceramic spheres (2 mm OD) was placed in order to preheat the gas feed. The furnace temperature

was kept within a maximum variation of 2°C by an automatic temperature controller. The gas exiting the reactor was led to a condenser to remove steam. The remaining components were continuously analyzed by non-dispersive infrared (CO and CO_2), flame ionization (HC), magnetic susceptibility (O_2), and chemiluminiscence (NO_x).

In order to investigate the TWC behavior of the prepared samples in an environment which resembled the exhaust *A*/*F* fluctuations in a closed-loop emission control system, we used a similar apparatus as that developed previously by Schlatter et al. [5]. Two fast-acting solenoid valves allowed one to cycle between the following two feedstreams prepared in two independent gas blending systems:

Reducing feedstream (*A*/*F*=14.13). It was composed of 10% CO_2, 1.60% CO, 900 ppm NO, 900 ppm C_3H_6, 0.465% O_2, 10% H_2O, and a balance of N_2.

Oxidizing feedstream (*A*/*F*=15.17). It consisted of 10% CO_2, 0.40% CO, 900 ppm NO, 900 ppm C_3H_6, 1.26% O_2, 10% H_2O, and a balance of N_2.

The redox characteristics of the model gas mixtures can be identified by the air-to-fuel ratio fed to the engine, *A*/*F*, which can be expressed as a function of the concentration of the different components in the feedstream. When C_3H_6 is used as hydrocarbon and no H_2 is present in the feedstream, *A*/*F* is given by

$$\frac{A}{F}=\frac{14.63}{1+0.02545\{[CO]+9[C_3H_6]-2[O_2]-[NO]\}} \quad (1)$$

When *A*/*F* is below, equal to or above 14.63, the reduction character of the gas mixture is reducing, stoichiometric or oxidizing, respectively.

The prepared catalysts were tested by cycling the reducing and oxidizing feedstreams, with a frequency of 1 Hz, an amplitude of ±0.5 *A*/*F*, and a space velocity of 125 000 h^{-1} (STP). The temperature was increased from 100 to 600°C at a rate of 3°C min^{-1}, and the conversion data were continuously measured. Thus, the *light-off temperature* which is necessary to achieve 50% conversion, T_{50}, and the stationary *conversion at the normal running temperature* of 500°C, X_{500}, were determined from the obtained activity data.

Once the conversion-temperature profiles was obtained, the experiment was continued at 500°C, but shifting the cycled feedstream to some stationary feedstreams with the following compositions: 10% CO_2, 900 ppm NO, 900 ppm C_3H_6, 10% H_2O, CO and O_2 as specified in Table 3, and a balance of N_2. These different CO and oxygen percentages in the feedstream allow us to experiment with different *A*/*F* values: 14.13, 14.33, 14.53, 14.63, 14.73, 14.93, and 15.13. From these experiments one can determine the *stoichiometric window*, defined as the interval of *A*/*F* inside which the conversion is equal to or above 70% for all the three pollutants.

Table 3
CO and O_2 concentration in stationary feedstreams of experiments at 500°C (vol.%)

	I	II	III	IV	V	VI	VII
CO	1.6	1.0	1.0	1.0	1.0	1.0	1.0
O_2	0.465	0.448	0.724	0.860	0.993	1.254	1.510
A/*F*	14.13	14.33	14.53	14.63	14.73	14.93	15.13

3. Results and discussion

3.1. Effect of aging on light-off curves

Table 4 shows how the textural properties of the ceria-modified alumina are changed by the thermal aging treatment at high temperature. The textural evolution of the mono- and multi-metallic catalysts with aging was similar to that of the promoter-modified support, which is not surprising considering the low metallic contents. A 41% decrease of the BET surface area with aging is observed. The pore volume is consequently reduced and the pore size increased. Perrichon et al. [6] reported a loss in surface area of ceria with thermal aging, causing reduction of the microporous surface and subsequent sintering of the ceria particles with possible reduction of the oxygen storage capacity and, as a consequence, modification of the catalyst activity.

Table 4
Textural properties of aged and fresh ceria-modified alumina

	Aged	Fresh
Surface area BET ($m^2\,g^{-1}$)	107	181
Pore volume ($cm^3\,g^{-1}$)	0.71	0.84
Average pore radius (nm)	13.7	9.5
Mode pore radius (nm)	8.6	6.1

The activity of the fresh mono- and multi-metallic catalysts has been reported elsewhere [3]. There, it was shown how all fresh palladium-containing catalysts presented similar light-off curves, no matter the nature of the other metal or metals present, together with palladium, in the catalyst. Hence, the results in this section are presented analyzing first the light-off curves obtained for the catalysts which do not contain palladium, and then for those containing palladium.

Figs. 1 and 2 show that, after thermal aging, all catalysts maintain a high activity at 500°C. Considering the results of Table 4, this means that the textural modifications induced by aging do not greatly affect catalyst activity at normal operation temperature. Reduction of specific surface area and pore volume are mainly due to occlusion of the small internal pores of the support, where only small amounts of ceria or noble metals would be deposited.

Fig. 1 shows the conversion vs. temperature curves obtained for CO, NO and C_3H_6 with fresh and aged

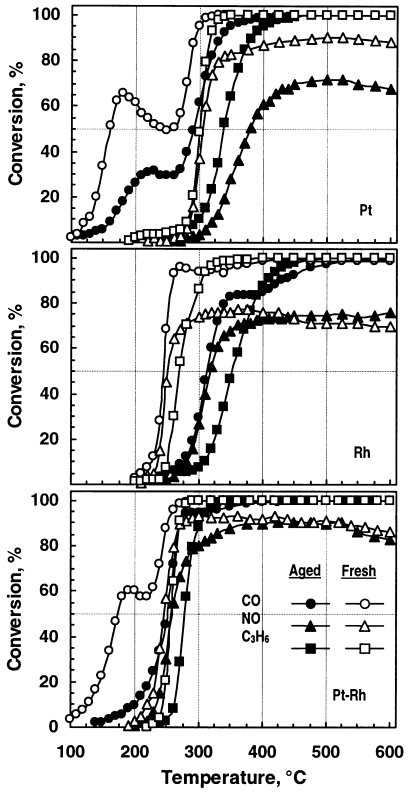

Fig. 1. Light-off curves corresponding to fresh and aged Pt, Rh and Pt–Rh catalysts.

Pt, Rh and Pt–Rh catalysts in the activity essays at programmed temperature. Fig. 2 shows those corresponding to Pd-containing mono- and multi-metallic catalysts (Pd, Pd–Pt, Pd–Rh, Pd–Pt–Rh). Tables 5 and 6 list the values of T_{50} and X_{500}, respectively, corresponding to the experiments shown in both figures.

Table 5 shows significant differences between fresh and aged samples. Thermal aging of NM/CeO_2/Al_2O_3 (NM: noble metal) catalysts, in the presence of steam, causes sintering of both ceria and noble metals. This reduces the interaction between both components, thus inhibiting the cyclic change between the oxidation states of cerium and decreasing the oxygen storage capacity [7,8]. The loss of interface between noble metals and ceria is mostly responsible for the changes in activity observed in Table 5 [8,9].

Fig. 1 and Table 6 show that the mono-metallic Pt catalyst presents no change in CO and C_3H_6 conversion at 500°C before and after aging, both of them being 100%. NO conversion, however, decreases from 90 to 72% after aging. Light-off temperatures, in Table 5, increase for the three pollutants with aging: 45°C for CO, 73°C for NO and 38°C for C_3H_6. Moreover, CO conversion at temperatures below 200–225°C decreases significantly after aging.

Platinum sintering has been reported to start around 800°C [9], the sintering process being quicker in oxidizing than in reducing conditions [10]. Thus, deactivation of platinum catalysts when aging is carried out in stoichiometric feedstreams is intermediate to that observed in oxidizing or reducing feedstreams [11].

The mono-metallic Rh catalyst presents (Table 5) an increase in light-off temperatures after aging of, 68°C for CO, 65°C for NO and 85°C for C_3H_6. However, Table 6 and Fig. 1 show that very small differences are observed in the conversion values at 500°C for the three pollutants. Deactivation of the rhodium catalyst after redox cycled aging is smaller than that obtained after a similar thermal treatment in oxidizing conditions. Rhodium particles are sintered at high temperature in oxidizing conditions, but a reduction treatment at high temperature can redisperse the metal [12,13].

The bimetallic Pt–Rh catalyst remains very active for the removal of CO, NO and C_3H_6 after aging: no change is observed in the conversion between fresh and aged samples at 500°C, the conversion being always above 90% for the three pollutants (Table 6). Besides, the light-off temperatures of the aged

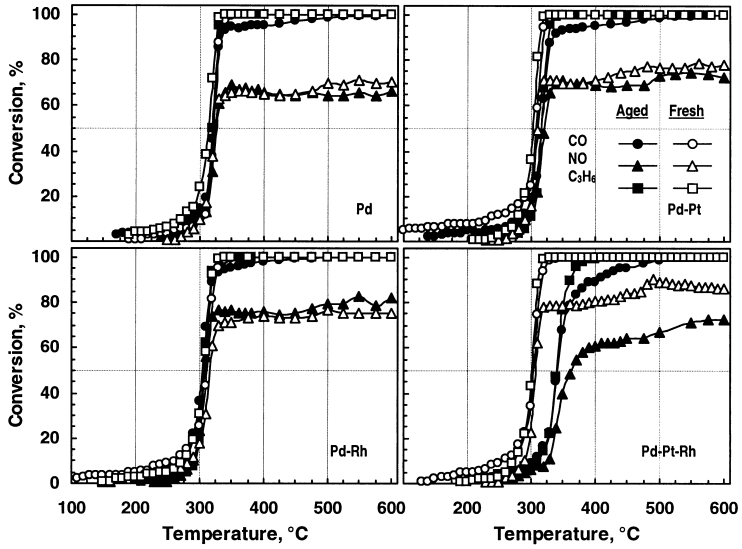

Fig. 2. Light-off curves corresponding to fresh and aged palladium-containing mono- and multi-metallic catalysts.

Pt–Rh catalyst are always well below those of the mono-metallic Pt and Rh catalysts subjected to similar aging and, what is more interesting, quite close to those of the fresh mono-metallic Rh catalyst. This synergistic effect between platinum and rhodium can be explained if we consider that aging takes place similarly in mono- and bi-metallic catalysts. If there is a Pt–Rh alloy in the fresh bimetallic catalyst, both phases are segregated during aging [3,14]. Also, diffusion of H_2 or CO adsorbed on Pt facilitates redispersion of rhodium particles at lower temperatures than those required when platinum is absent [15,16].

The light-off curve for CO obtained with the Pt–Rh catalyst (Fig. 1) shows how the catalyst keeps a part of its activity to oxidize CO at temperatures below 200–225°C, after aging, a feature characteristic of the platinum catalyst. The Pt–Rh catalyst aged in redox cycled feedstream shows a behavior close to that of the fresh Rh catalyst due to regeneration of oxidized Rh particles during the rich cycle by the presence of Pt.

The aged mono-metallic Pd catalyst presents a very small decrease in activity compared to the fresh sample (Fig. 2), which is also observed by the small change of T_{50} values for the three pollutants in Table 5, with a maximum increase of 6°C for C_3H_6. Concerning conversions at 500°C (Table 6), the values are nearly identical for fresh and aged samples, the maximum

Table 5
Light-off temperatures, T_{50} (°C), of aged and fresh catalysts

Catalyst	CO		NO		C_3H_6	
	Aged	Fresh	Aged	Fresh	Aged	Fresh
Pd	321	322	326	325	320	314
Pt	290	255	379	306	338	300
Rh	313	245	318	253	353	268
Pd–Pt	316	307	321	310	316	303
Pd–Rh	304	312	308	316	307	307
Pt–Rh	252	173	258	247	277	257
Pd–Pt–Rh	342	304	363	307	341	301

Table 6
Conversions at 500°C, X_{500} (%), of aged and fresh catalysts

Catalyst	CO		NO		C_3H_6	
	Aged	Fresh	Aged	Fresh	Aged	Fresh
Pd	98	100	65	70	100	100
Pt	100	100	72	90	100	100
Rh	97	99	75	71	100	100
Pd–Pt	99	100	73	77	100	100
Pd–Rh	100	100	80	77	100	100
Pt–Rh	100	100	90	91	100	100
Pd–Pt–Rh	98	100	67	89	100	100

difference found for NO, with a 5% decrease after aging.

Although the aged Pd catalyst presents similar CO and C_3H_6 conversions at 500°C as the fresh catalyst, about 100% (Table 6), the fresh sample reaches this 100% conversion at lower temperature, 340°C (Fig. 2) than the aged sample, about 500°C. Both fresh and aged Pd catalysts present C_3H_6 conversions above those of CO.

The palladium present in the catalyst may have been sintered during thermal aging. The rate of sintering of a metal supported on a porous support depends on its mobility, which is related to the partial pressures of the species present on the surface [17]. According to this, sintering of palladium particles at high temperature will be quicker in reducing environment because of the high vapor pressure of metallic palladium compared to PdO. Several authors confirm this fact [18,19], showing that relatively high palladium dispersion on high surface area supports can be preserved after several hours of treatment in air at 900°C [20]. According to this reasoning, the sintering suffered by the catalyst aged under redox cycled feedstream should be lower than that suffered by the catalyst aged in reducing feedstream, as half of the time is submitted to a less aggressive environment. Changes in the structure were confirmed experimentally by XRD and HREM [21], and the formation of new active mixed phases was observed.

Bimetallic Pd–Pt and Pd–Rh catalysts aged under these conditions show similar behavior as the aged mono-metallic Pd catalyst. However, Pd–Pt–Rh catalyst presents an important deactivation after aging, showing higher light-off temperatures and lower conversions at 500°C.

3.2. Effect of aging on stoichiometric windows

Fig. 3 shows the stoichiometric windows corresponding to Pd, Pt, Rh and Pt–Rh catalysts, both fresh and after aging. Table 7 lists the amplitude of the stoichiometric windows, the upper and lower *A*/*F* limits, as well as the reactant responsible for this limit.

The upper limit of the stoichiometric window is always fixed by NO conversion in oxidizing conditions, no matter what the catalyst composition is. The aging treatment modifies this value very little. More important changes are observed in the lower limit, with CO and C_3H_6.

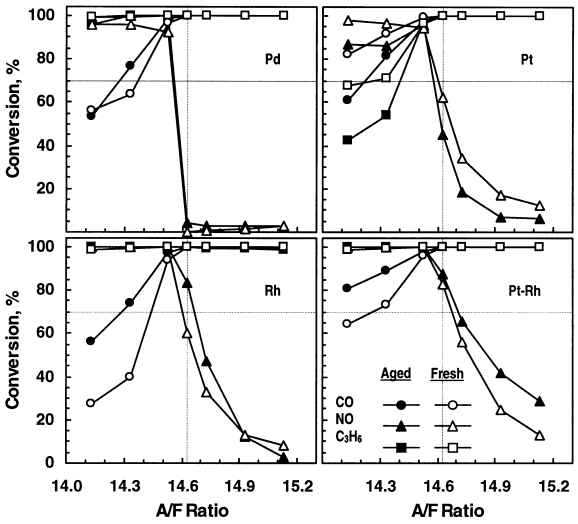

Fig. 3. Stoichiometric windows corresponding to fresh and aged Pd, Pt, Rh and Pt–Rh catalysts.

The aged Pt catalyst shows lower C_3H_6 conversion in reducing conditions (Fig. 3), due to its lower capacity to produce steam reforming. This produces a shift in the lower limit of the window to higher *A*/*F* values compared to the fresh sample, thus decreasing the amplitude of the stoichiometric window. However, aged Rh and Pt–Rh catalysts produce C_3H_6

Table 7
Stoichiometric windows of aged and fresh catalysts

		Limits	Amplitude
Pd	Aged	$14.27^{(CO)}$–$14.56^{(NO)}$	0.29
	Fresh	$14.37^{(CO)}$–$14.53^{(NO)}$	0.16
Pt	Aged	$14.40^{(HC)}$–$14.58^{(NO)}$	0.18
	Fresh	$14.26^{(HC)}$–$14.61^{(NO)}$	0.35
Rh	Aged	$14.29^{(CO)}$–$14.67^{(NO)}$	0.38
	Fresh	$14.44^{(CO)}$–$14.60^{(NO)}$	0.16
Pd–Pt	Aged	$14.26^{(CO)}$–$14.56^{(NO)}$	0.30
	Fresh	$14.13^{(CO-HC)}$–$14.56^{(NO)}$	0.43
Pd–Rh	Aged	$14.24^{(CO)}$–$14.56^{(NO)}$	0.32
	Fresh	$14.13^{(CO-HC)}$–$14.56^{(NO)}$	0.43
Pt–Rh	Aged	$14.13^{(CO-HC)}$–$14.71^{(NO)}$	0.58
	Fresh	$14.26^{(CO)}$–$14.68^{(NO)}$	0.42

conversions close to 100% with all feedstreams, even in highly reducing conditions.

The NO conversion of the aged platinum catalyst is lower than that of the fresh one, even in reducing conditions, although it hardly affects the amplitude of the stoichiometric window. Aged Rh and Pt–Rh catalysts present better NO conversion than when fresh, thus shifting the upper limit of the stoichiometric window to higher A/F values.

The water gas shift reaction significantly contributes to CO conversion in reducing conditions. As for C_3H_6, CO conversion in reducing conditions decreases with Pt catalyst after aging, due to the lower capacity of platinum to react with steam. Aged Rh and Pt–Rh catalysts present higher activity for CO in reducing conditions than the fresh samples, due to the contribution of water gas shift.

The stoichiometric windows corresponding to the palladium catalyst in Fig. 3 show that the behavior is very similar, either fresh or aged, in stoichiometric or oxidizing conditions, with CO and C_3H_6 conversions close to 100%, and practically no NO conversion. However, NO conversion in reducing conditions is always close to 100% with the aged Pd catalyst, while conversions of CO and C_3H_6 are very similar with both fresh and aged samples.

Palladium-containing multi-metallic catalysts (Table 7) present stoichiometric windows very similar to those of the mono-metallic Pd catalyst. The presence of Pt and/or Rh in the formulation does not seem to produce any positive effect in the aged samples.

4. Conclusions

All the catalysts completely oxidized both CO and C_3H_6, even after being subjected to the thermal aging treatment. Aging partially decreases NO conversion, being mono- and bimetallic Rh-containing catalysts that support better aging treatment. Conversions above 65% were achieved with all the aged samples.

Pd is the mono-metallic catalyst more resistant to aging, followed by Pt and Rh. This effect can also be found in the bimetallic formulations containing palladium, i.e. Pd–Pt and Pd–Rh being much more resistant than the Pt–Rh catalyst, although the latter is the most active even after subjected to the thermal aging treatment.

The Pt–Rh formulation amplifies the stoichiometric windows after aging. This effect seems to be related to the presence of Rh, as the width of the stoichiometric window for the mono-metallic Pt catalyst significantly decreases with aging. The Pt–Rh formulation shows a synergistic effect that amplifies the width of the stoichiometric window compared to that of the individual metals, particularly after aging.

All Pd-containing catalysts present similar stoichiometric windows after aging, no matter the metal accompanying the palladium in the catalyst, with a width close to that of the mono-metallic Rh catalyst.

This behavior of the prepared formulations can be explained in terms of the impact of the interactions between metals and/or cerium oxide [21] and could provide a valuable basis for designing new formulations with enhanced characteristics.

Acknowledgements

The authors wish to acknowledge financial support from Universidad del País Vasco/EHU (UPV069.310-G40/98) and Ministerio de Educación y Cultura (MAT98-0971).

References

[1] G.C. Koltsakis, A.M. Stamatelos, Progr. Energy Combust. Sci. 23 (1997) 1.
[2] R.J. Farrauto, R.M. Heck, Catal. Today 51 (1999) 351.
[3] J.R. González-Velasco, J.A. Botas, R. Ferret, M.A. Gutiérrez-Ortiz, Studies in Surface Science and Catalysis, Vol. 116 (CAPoC IV), Elsevier, Amsterdam, 1998, p. 73.
[4] J.R. González-Velasco, J.A. Botas, J.A. González-Marcos, M.A. Gutiérrez-Ortiz, Appl. Catal. B 12 (1997) 61.
[5] J.C. Schlatter, R.M. Sinkevitch, P.J. Mitchell, Ind. Eng. Chem. Prod. Res. Dev. 19 (1980) 288.
[6] V. Perrichon, A. Laachir, S. Abouarnadasse, O. Touret, G. Blanchard, Appl. Catal. A 129 (1995) 69.
[7] E. Rogemond, R. Fréty, V. Perrichon, M. Primet, M. Chevrier, C. Gauthier, F. Mathis, Appl. Catal. A 156 (1997) 253.
[8] S.J. Schmieg, D.N. Belton, Appl. Catal. B 6 (1995) 127.
[9] T. Huizinga, J. Van Grondelle, R. Prins, Appl. Catal. 10 (1984) 199.
[10] D.D. Beck, C.J. Carr, J. Catal. 110 (1988) 285.
[11] R. Rohé, V. Pitchon, G. Maire, Studies in Surface Science and Catalysis, Vol. 116 (CAPoC IV), Elsevier, Amsterdam, 1998, p. 147.
[12] D.D. Beck, C.J. Carr, J. Catal. 144 (1993) 296.

[13] J.A. Botas, J.I. Gutiérrez-Ortiz, M.A. Gutiérrez-Ortiz, J.R. González-Velasco, in: Proceedings of the 16th Simposio Iberoamericano de Catálisis, Cartagena de Indias, Colombia, August 1998.
[14] J.A. Botas, R. Ferret, M.A. Gutiérrez-Ortiz, J.R. González-Velasco, J. Chim. Phys. 12 (1999) 437.
[15] Z. Hu, F.M. Allen, C.Z. Wan, R.M. Heck, J.J. Steger, R.E. Lakis, C.E. Lyman, J. Catal. 174 (1998) 13.
[16] C. Howit, V. Pitchon, G. Maire, J. Catal. 154 (1995) 47.
[17] J. Barbier Jr., D. Duprez, Appl. Catal. B 4 (1994) 105.
[18] H. Sinjoh, H. Muraki, Y. Fujitami, Studies in Surface Science and Catalysis, Vol. 71 (CAPoC II), Elsevier, Amsterdam, 1991, p. 617.
[19] W. Zou, R.D. González, Appl. Catal. A 126 (1995) 351.
[20] R.F. Hicks, H. Qi, M.L. Young, R.G. Lee, J. Catal. 122 (1990) 279.
[21] J.R. González-Velasco, M.A. Gutiérrez-Ortiz, J.A. Botas, S. Bernal, J.M. Gatica, J.A. Pérez-Omil, Studies in Surface Science and Catalysis, Vol. 126 (Catalyst deactivation), Elsevier, Amsterdam, 1999, p. 187.